CHEMICAL ENGINEERING TRANSACTIONS
VOL. 89, 2021
A publication of AIDIC
The Italian Association of Chemical Engineering
Online at www.cetjournal.it
Guest Editors: Jeng Shiun Lim, Nor Alafiza Yunus, Jiří Jaromír Klemeš

ISBN 978-88-95608-87-7; **ISSN** 2283-9216
DOI: 10.3303/CET2189108

Photocatalytic Activity of Nanoparticles TiO_2-P25@n-TiO_2 Composite in Gas Phase

Guy Didier Fanou[a], Mamadou Traore[b,*], Benjamin Kouassi Yao[a], Khay Chhor[b], Andrei Kanaev[b]

[a]Laboratoire des Procédés de Synthèse, de l'Environnement et des Energies Nouvelles, LAPISEN, INP-HB, Côte d'Ivoire
[b]Laboratoire des Sciences des Procédés et des Matériaux, LSPM-CNRS UPR 3407, Institut Galilée, Université Sorbonne Paris Nord
traore@lspm.cnrs.fr

Stable TiO_2-P25@n-TiO_2 nanocoating was prepared based of grafted size selected 5 nm Titanium-oxo-alkoxo (n-TiO_2) nanoparticles on P25-TiO_2 nanoparticles surface and their immobilization on Aluminium substrate. The 5-nm oxo-TiO_2 particles were prepared in a sol-gel reactor with rapid reagents micromixing. The photocatalytic test of ethylene degradation, in a continuous-flow fixed bed reactor, showed an increase of the photocatalytic yield with number of the deposited layers until a sursaturation regime. By modeling the photocatalytic activity of the composite, a death layer of electron-hole pairs excitation of 20 nm, corresponding of the film thickness, was found. Furthermore, the estimation of the TiO_2 absorption coefficient ($k \leq 2 .10^4$ cm^{-1}) indicates a strong porosity of the deposited films.

1. Introduction

The water and air quality is decreasing which represents a serious threat for all living species. Among the possible techniques for the destruction of pollution traces are the Advanced Oxidation Technologies (TOA). From 2000 to 2018, the number of publications on TOA increases by more than fourfold and reaches 7000 publications (Giwa et al, 2021). The most common and low cost photocatalyst used in this technique is the commercial titanium dioxide TiO_2-P25 mainly due to its interesting electrochemical and photocatalytic properties that are largely applied in the field of photocatalysis (Fujishima et al, 2008 ; Fujishima et al, 2000 ; Hurum et al, 2003; Lasa et al, 2005; Linesbigler et al, 1995; Malato et al, 2002; Ohko et al, 1997; Tompkins et al, 2005; Wang et al, 1998). However, films prepared with this photocatalyst suffer from the poor adhesion of deposit caused by the low chemical reactivity of TiO_2-P25 large particle size (~ 30 nm).To improve mechanical properties of photocatalytic films, Fanou et al (2016) proposed to fabricate new composite TiO_2-P25@n-TiO_2 photocatalyst, in which the TiO_2-P25 particles are bound to the glass substrate via titanium-oxo-alkoxy bonds (n-TiO_2). n-TiO_2 is obtained via a sol–gel reactor with turbulent mixing of reactive fluids (Azouani et al, 2010a; Rivallin et al, 2005) permitted us to control the chemical reactions and stabilizing monodispersed sols of a very small size : 2.0 nm, 3.2nm and 5.2nm diameters (Azouani et al, 2007).
In this work, the photocatalytic activity of this new composite is reported, excepted that aluminum is use as substrate instead of glass. Aluminum was chosen as a support because of its good mechanical strength and its high performance against corrosion. For some practical liquid or gaseous depollution applications, these properties play an important role as photocatalysts are likely to be handled more often and used in polluted environments such as wastewater, corrosive gases etc. Structural properties of the TiO_2-P25@n-TiO_2 films, yield of ethylene photo-degradation in a fixed-bed continuous-flow reactor and a photoactivity modeling are reported.

Paper Received: 25 May 2021; Revised: 20 September 2021; Accepted: 7 November 2021
Please cite this article as: Fanou G.D., Traore M., Yao B.K., Chhor K., Kanaev A., 2021, Photocatalytic Activity of Nanoparticles TiO_2-P25@n-TiO_2 Composite in Gas Phase, Chemical Engineering Transactions, 89, 643-648 DOI:10.3303/CET2189108

2. Material and methods

2.1 Elaboration of TiO_2-P25@n-TiO_2 films

The general approach to synthesize the TiO_2-P_{25}@n-TiO_2 has been proposed by Fanou et al. (2016). The sol nanoparticles are prepared in the sol–gel reactor using titanium tetraisopropoxide (TTIP) as a precursor. Two stock solutions: 50 cm^3 of a TTIP/propan-2-ol solution and 50 cm^3 of a H_2O/propan-2-ol solution, was synchronously injected under nitrogen into the turbulent mixing zone (Re = 4500) of sol–gel reactor (Azouani et al. 2010b) where the oxo-TiO_2 nanoparticles were generated from hydrolysis condensation reactions. The particle size can be tuned by adjusting the hydrolysis ratio H = C_{H2O}/C_{TTIP}, where C_{H2O} and C_{TTIP} are respectively water and titanium precursor concentrations. We have prepared colloids using hydrolysis ratio H = 2, which corresponds to one of stability domains of the sol–gel process and enables particles size of 5.2 nm (Azouani et al. 2007). The suspended oxoparticles solution was subsequently transferred to a glove box LABstar MBraun where they were combined slowly with TiO_2-P25 powder under stirring. The ratio 66 % of TiO_2-P25/ n-TiO_2 was the same for all prepared samples.Then photocatalyst particles are immobilized on the aluminum shavings which are supplied by the company Sigma-Aldrich in the form of a wire of 1 mm in diameter with a purity of 99.7%. A very thin native layer of alumina (5-10 nm thickness) is on their surface. Before putting it in contact with the colloids for the dip-coating, the aluminum wire is cut into small pieces of 1.5 to 3 mm in length and then annealed in air at 300 ° C for 2 h (Kokubo et al, 1990). This surface treatment increases the thickness of the aluminum oxide oxidation layer promoting the formation of hydroxyl groups (-OH) on the surface of the substrate. Each TiO_2-P25@n-TiO_2 layer consists in putting aluminum shaving inside a sol previously obtained during 10 minutes before a thermal treatment at 450°C during 4 hours.

2.2 Photocatalyst characterization

The prepared samples were structurally characterised by X-ray diffraction XRD (INEL XRG 3000) using CuKα radiation with Nickel filter. Raman spectra were measured at 516 nm using micro-Raman high-resolution HR800 installation (HORIBA JobinYvon) with the spectral and spatial resolution respectively 0.25 cm−1 and 5 µm. The scattered light is collected by Peltier cooled CCD camera in a backscattering configuration. The study of the thermal behaviours and specific surface of the samples were respectively carried out on a SETARAM TG-DTA 92 device and a Coulter SA3100 device.The photocatalytic activity of the prepared samples was tested in a continuous-flow fixed-bed reactor on ethylene decomposition. A gas flow of pollutant (120 ppm) mixture with dry air and flow rate of 7.5 mL/min passes through a reactor tube of 6-mm diameter made of glass transparent in the UV-A spectral range [16, 17]. The glass beads coated photocatalyst samples were filled the reactor tube of 15 cm length. The tube is surrounded at a radial distance of 3 cm by six 8-W lamps emitting at 362 nm (Δλhwfm = 22 nm). The reactor temperature 46 ± 2 °C was maintained during the experiments. Ethylene concentrations before (Cin) and after (Cout) the photocatalytic reactor were monitored by online gas chromatography (Varian 191 CP 3800) equipped with a capillary column (HP-PLOT/Q) and a flame ionization detector FID. Two injection loops of 250 µL and heated at 80 °C allow measurements of pollutant concentration in continuous mode. The reactor yield (or ethylene conversion) is calculated according to the formula: η(%) = (Cin-Cout)/Cin×100. The column temperature and flow rate of the carrier gas (N2) were respectively 50 °C and 5 mL/min.

3. Results and discussions

3.1 Thermal analysis

Thermal studies were performed with TiO_2-P25@n-TiO_2 powder obtained with 40wt% of TiO_2-P25 loading.The results of differential thermal (DTA) and thermogravimetric (TGA) analyses are shown in Figure **1**.
The quasi total mass loss was observed in the temperature range between 60 and 350 °C. This is attributed to departures of physically adsorbed solvent molecules, burning of the organic residues as well as the condensation of nonhydrolysed alkoxy groups (Amores et al, 1995 ; Rodriguez-Talavera et al, 1997). The crystallization of the anatase phase is associated with the exothermic peak at 379 °C on ATD curve which is markedly low compared to that of pure TiO_2 observed usually around 400 °C. According to Kumar *et al*., 1992 crystallites nucleation and growth take place at this point and the presence of TiO_2-P25 anatase in the composite can reduce the activation energy and promote the crystallisation process by decreasing the onset temperature.

3.2 Raman and X-Ray Diffraction Analyses

Raman spectrum of the composite powder is shown in Figure **2a**. Several strong peaks are observed at 144, 400, 518 and 639 cm^{-1} for the anatase phase and are respectively attributed to vibrational modes Eg, B1g,

A1g, Eg. The small amount rutile phase in TiO_2-P25@n-TiO_2 composite gives a weak rise of shoulders, the most intense of which appear at 443 and 610 cm-1 due to Eg and A1g modes (Balachandran et al, 1982).

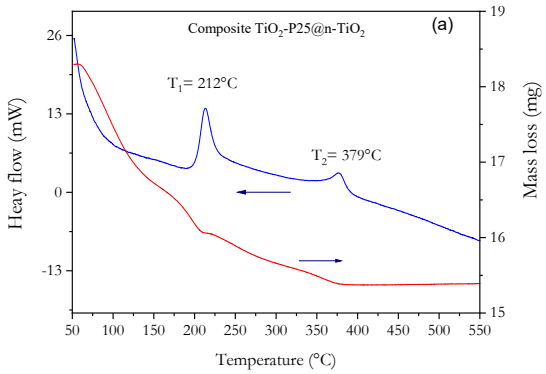

Figure 1: DTA-TGA curves of TiO_2-P25@ n-TiO_2 composite. The oxo-TiO_2 preparation conditions are: CTTIP = 0.15 M, H =2, T = 20 °C, Re = 4500

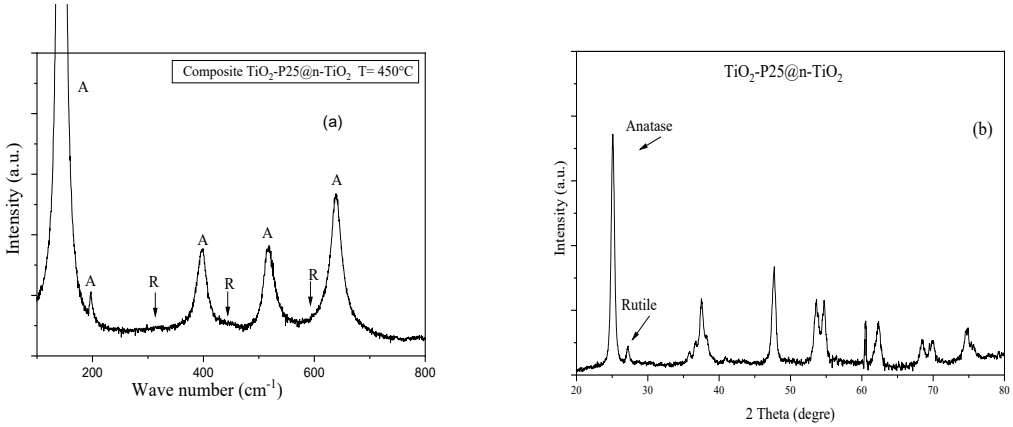

Figure 2 : Raman spectra (a) and XRD Diagrams (b) of TiO_2-P25@n-TiO_2 composite prepared with H = 2, r = 65% treated at 450 °C. A and R denote the anatase and rutile phases respectively

Figure 2b illustrated X-ray diffraction pattern of prepared powder like sample. The patterns of the coatings and powders are expected to be quite similar since, according to Martyanov and Klabunde (Martyanov et al, 2004), the substrate has little influence on the anatase phase crystallization, while can significantly increase the anatase-rutile transition temperature. Two principal RX diffraction peaks are observed at 25.07 and 27.25 ° respectively assigned to anatase (101) and rutile (110).Their intensity ratio (anatase/rutile) is much larger compared to the original pure TiO_2-P25 qualitatively indicating the presence of n-TiO_2 anatase phase in the composite.

3.3 Photocatalytic activity

The photocatalytic performance of the materials was evaluated by photodegradation of ethylene using a fixed bed tubular reactor in continuous mode. The measurements were carried out using excitatory length λ = 360 nm. The light is turn on 10 minutes after the beginning of the run. Figure 3 exposes the obtained results.
The curves show that the thickness of the film has a great influence on its photocatalytic activity. Conversion of ethylene increases with the number of layers. The average variation of the conversion η between the layers seems to be regular around 15%. This result, in agreement with that reported by many authors for TiO_2 coatings on glass (Heikkala et al, 2009; Jung et al, 2002; Nielsen et al, 2012), can be attributed to the increase of the specific surface area of the films making it possible to increase the active sites. The BET measurements carried out on the samples of 1, 3 and 7 layers from the adsorption-desorption isotherms of nitrogen are presented in Table 1.

Table 1: BET Specific surface area of samples

Samples	Aluminum without layer	1 layer	3 layers	7 layers
Specific Area ($m^2.g^{-1}$)	0.004	0.046	0.103	0.275

For one layer, ethylene conversion yield obtained with aluminum substrate is 5 times lower than that obtained with an equivalent film deposited on a borosilicate glass substrate (Fanou et al, 2016). This reduction corroborates the result of Ho et al., 2007 on the comparison study of the photocatalytic efficiency of TiO_2 films on aluminum and on quartz. Different factors can be put forward to explain this result:

- the amount of photocatalyst fixed on the metal substrate by sol-gel is low compared to films on borosilicate glass rich in silica : the bonds ensuring the adhesion of films by dip-coating result from the condensation of the Si-OH and Al-OH groups of the substrate and the Ti-OH group of the composite. This reaction is easily carried out between the Ti-OH and Si-OH groups because of the basic nature of the first and acidic of the second. On the contrary, the Al-OH group is an amphoteric, consequently the condensation with Ti-OH is relatively less easy.
- Numerous previous studies have shown that Al^{3+} ions from the composite-substrate interface can diffuse inside of TiO_2 films (Zhu et al, 2001; Lopez et al, 2013; Ho et al., 2007) thus forming a cationic Al-TiO_2 doped material. This type of doping has a negative effect on the photocatalytic activity because the dopant acts as a recombination center for photoinduced charges (e- / h +) (Gesenhues, 2001; Lee et al, 2003).

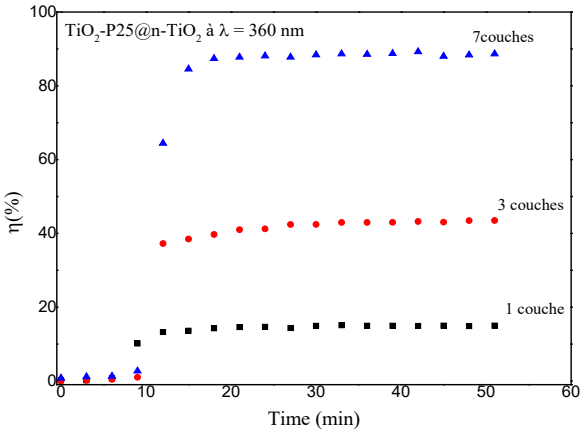

Figure 3 : Evolution of the photodegradation of ethylene by TiO_2-P25@n-TiO_2 composite as a function of the run time for 3 layer thickness. (λ = 360 nm, ethylene 150 ppm, flow rate 10 mL.min^{-1}).

3.4 Modeling

The material photocatalytic efficiency generally depends on its charge. It tends towards a saturation regime which will be established when the materials can no longer absorb more the photons of the exciting radiation. This occurs when the mass is large, for high film thickness (Hermann, 1999).

Figure 4 : Schematic representation of the layer

The light intensity in the layer (L) can be expressed by the following equation:

$$L = I_0 e^{-k(\delta - x)} + R I_0 e^{-k\delta} e^{-kx} \quad (1)$$

Where I_0 is incident light intensity, R is reflection coefficient from Al plate, δ is film thickness and k is photodegradation rate constant.
The probability of charges (e/h) survival as distance from substrate is given by the following equation

$$P = \left(1 - e^{-\frac{x}{a}}\right) \quad (2)$$

where *a* is death layer for electron-hope pairs excitation.
The layer charge is a combination between absorbed light and probability of charges migration to the surface:
$N_{e/h} \propto$ (absorbed light) x (probability of charges migration to surface) $\equiv \int L(x)P(x)dx$, $0 \leq x \leq \delta$ (3)
Finally the photocatalytic activity can be defined by Activity $\equiv A = \int kL(x)P(x)dx$, with $x \in [0, \delta]$ (4)
Fanou et al (2016) showed that the average order of the photooxidation reaction is close to 1 for ethylene concentrations ≤ 120 ppm. Consequently, the photocatalytic activity can be written:

$$A = I_0[\left(1 - e^{-k\delta}\right) - (1 - ka)^{-1}\left(e^{-k\delta} - e^{-\frac{\delta}{a}}\right)] + RI_0e^{-k\delta}[\left(1 - e^{-k\delta}\right) - (1 - ka)^{-1}\left(1 - e^{-k\delta - \frac{\delta}{a}}\right)] \quad (5)$$

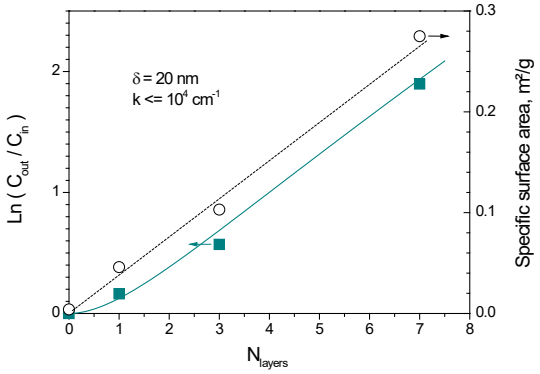

Figure 5 : Fit of experimental data adapted to a continuous-flow-fix-bed reactor

Most important result of the best fit of experimental data (figure 5) with equation 5 is that *a*=20 nm. This adaptation layer has a poor photocatalytic activity because of the electronic coupling with substrate. The aluminium plate attracts photoinduced charges, which recombine. Apparently, the thin oxidized surface layer of the plate does not effectively separate semiconductor and metal.
This is not an effect of the specific surface area (BET), since the last is proportional to the deposited mass (N_{layers}) (see Figure 5). Furthermore, no signs of saturation permit an estimation of the TiO_2 absorption coefficient at 360 nm: $k \leq 2 \cdot 10^4$ cm^{-1}, which indicates a strong porosity of the deposited films. Indeed, the value of $k \sim 10^5$ cm^{-1} could be expected in TiO_2 solid, which sets the film mass density on ~20% (or smaller) of the bulk solid. Generally, 50% bulk mass density is expected in sol-gel films. Even lower mass density of the prepared films can be explained by the particular composition of P25 nanopowder particles linked by nano-TiO_2.

4. Conclusions

The photocatalytic performance of films deposited on aluminum was evaluated by photooxidation of ethylene at λ = 360 nm for the TiO_2-P25@n-TiO_2 composite. The results showed that the photocatalytic of the first layer of the deposit on Al is 5 times lower than that observed on borosilicate glass. This result was interpreted due to a lower mass deposition on the metal substrate resulting from less favorable condensation between the Ti-O-H and Al-O-H groups compared to that between Ti-OH and Si-OH. Finally, a modeling was carried out. A death layer of electron-hole pairs excitation of 20 nm, corresponding of the film thickness, was found. Furthermore, the estimation of the TiO_2 absorption coefficient ($k \leq 2 \cdot 10^4$ cm^{-1}) indicates a strong porosity of the deposited films.

References

Amores JMG, Escribano VS and Busca G., 1995 Anatase crystal growth and phase transformation to rutile in high-area TiO2, MoO3-TiO2 and other TiO2-supported oxide catalytic systems, J Mater Chem; 5: 1245-1249.
Azouani R, Soloviev A, Benmami M, Chhor K, Bocquet JF and Kanaev A, 2007. Stability and growth of titanium-oxo-alcoxy TixOy(OiPr)z clusters, J Phys Chem C; 111: 16243-16248.

Azouani R., Tieng S., Chhor K., Bocquet J.-F., Eloy P., Gaigneaux E. M., Klementiev K., Kanaev A., 2010, TiO2 doping by hydroxyurea at the nucleation stage: towards a new photocatalyst in the visible spectral range, Phys. Chem. Chem. Phys. 12 : 11325–11334.

Azouani R, Michau A, Hassouni K, Chhor K, Bocquet JF, Vignes JL et al., 2010 Elaboration of pure and doped TiO2 nanoparticles in sol-gel reactor with turbulent micromixing: application to nanocoatings and photocatalysis, Chemical Engineering Research & Design; 88: 1123-1130.

Balachandran U and Eror NG., 1982 Raman spectrum of titanium dioxide, J Solid State Chem; 42: 276-282.

Fanou G.D., Yao B., Cheng K., Brinza O., Traore M., Kanaev A., Chhor K., 2016, “Elaboration of novel nanoparticulate TiO2-P25@nTiO2 composite for Catalysis”, International Journal of Advanced Applied Physics Research 3 : 19-25.

Fujishima A, Rao TN and. Tryk DA, 2000. Titanium Dioxide Photocatalysis, J Photochem Photobiol C Photochem Rev; 1: 1-21.

Fujishima A, Zhang X and Tryk DA., 2008, TiO2 photocatalysis and related surface phenomena, Surf Sci Rep ; 63: 515-582.

Gesenhues U., 2001, Al-doped TiO2 pigments: influence of doping on the photocatalytic degradation of alkyd resins, J. Photochem. Photobiol. Chem. 139 243–251.

Giwa A., Yusuf A., Balogun H. A, Sambudi N. S., Bilad M. R., Adeyemi I., Chakraborty S. Curcio S., 2021, Recent advances in advanced oxidation processes for removal of contaminants from water: A comprehensive review, Process Safety and Environmental Protection, 146 : 220-256

Heikkilä M., Puukilainen E., Ritala M., Leskelä M., 2009, Effect of thickness of ALD grown TiO2 films on photoelectrocatalysis, J. Photochem. Photobiol. Chem. 204 200–208.

Herrmann J.-M., 1999, Heterogeneous photocatalysis: fundamentals and applications to the removal of various types of aqueous pollutants, Catal. Today. 53 115–129.

Ho W., Jimmy C.Y., Lee S., 2007, Photocatalytic activity and photo-induced hydrophilicity of mesoporous TiO2 thin films coated on aluminum substrate, Appl. Catal. B Environ. 73 135–143.

Hurum DC, Agrios AG, Gray KA, Rajh T and Thurnauer MC., 2003, Explaining the Enhanced Photocatalytic Activity of Degussa P25 Mixed-Phase TiO2 Using EPR, J Phys Chem B ;107: 4545-4549.

Jung K.Y., Park S.B., Ihm S.-K., 2002, Linear relationship between the crystallite size and the photoactivity of non-porous titania ranging from nanometer to micrometer size, Appl. Catal. Gen. 224 229–237.

Kokubo T., Kushitani H., Sakka S., Kitsugi T., Yamamuro T., 1990, Solutions able to reproduce in vivo surface-structure changes in bioactive glass-ceramic A-W3, J. Biomed. Mater. Res. 24 721–734.

Kumar KNP, Keizer K, Burggraaf AJ, Okubo T, Nagamoto H and Morooka S., 1992 Densification of nanostructured; titania assisted by a phase transformation, Nature; 358: 48-51.

Lasa HD, Serrano B and Salaices M., 2005, Photocatalytic reaction engineering, New York; USA: Springer Science; Business Media Inc.

Lee Y.C., Hong Y.P., Lee H.Y., Kim H., Jung Y.J., Ko K.H., Jung H.S., Hong K.S., 2003, Photocatalysis and hydrophilicity of doped TiO 2 thin films, J. Colloid Interface Sci. 267 127–131.

Linesbigler AL, Lu G and Yates JT., 1995, Photocatalysis on TiO2 surfaces. Principle mechanisms and and selected results, Chem Rev; 95: 735-758.

Lopez L., Daoud W.A., Dutta D., Panther B.C., Turney T.W., 2013, Effect of substrate on surface morphology and photocatalysis of large-scale TiO 2 films, Appl. Surf. Sci. 265 162–168.

Malato S, Blanco J, Vidal A and Richter C., 2002, Photocatalysis with solar energy at a pilot-plant scale: an overview, Appl Catal B Environ; 37: 1-15.

Martyanov IN and Klabundev. 2004, Comparative study of TiO2 particles in powder form and as a thin nanostructured film on quartz, J Catal; 225: 408-416.

Nielsen M.G., In S.-I., Vesborg P.C., Pedersen T., Almtoft K.P., Andersen I.H., Hansen O., Chorkendorff I., 2012, A generic model for photocatalytic activity as a function of catalyst thickness, J. Catal. 289 62–72.

Ohko Y, Hasimoto K and Fujishima A., 1997 Kinetics of photocatalytic reactions under extremely low intensity UV illumination on titanium dioxide thin films, J Phys Chem A ; 101: 8057-8062.

Rivallin M, Benmami M. Kanaev A and Gaunand A., 2005 Sol-gel reactor with rapid micromixing: modelling and measurements of titanium oxide nano-particles growth, Chemical Engineering Research & Design; 83: 67-74.

Rodriguez-Talavera R, Vargas S, Arroyo-Murillo R, Montiel-Campos R and Haro-Poniatowski E., 1997 Modification of the phase transition temperatures in titania doped with various cations, J Mater Res; 12: 439-443.

Tompkins DT, Lawnicki BJ, Zeltner WA and Anderson MA., 2005, Evaluation of photocatalysis for gas-phase air cleaning -Part1: Process; technical and sizing considerations, in:Geshwiler; M. (Ed.); Ashrae Transactions 111: 60.

Wang TM, Wang HY, Xu P, Zhao XC, Liu YL and Chao S., 1998, The effect of properties of semiconductor oxide thin films on photocatalytic decomposition of dyeing waste water, Thin Solid Films; 334: 103-108.

Zhu Y., Zhang L., Wang L., Tan R., Cao L., 2001, Interface diffusion and reaction between TiO2 film photocatalyst and aluminium alloy substrate, Surf. Interface Anal. 32 218–223.